



Viscosity Correlation for Aqueous Lithium Bromide Solution

Christian Fleßner¹  · Felix Ziegler¹

Received: 20 July 2022 / Accepted: 21 October 2022 / Published online: 2 December 2022
© The Author(s) 2022

Abstract

A correlation for dynamic viscosity of aqueous lithium bromide solution is proposed. The correlation is based on an empirical approach accounting for physical limitations. The data are compiled from 11 sources over a temperature range from $-20\text{ }^{\circ}\text{C}$ to $110\text{ }^{\circ}\text{C}$ and from pure water to salt mass fractions of 65 %. The correlation succeeds in predicting the solution's viscosity over the chosen range of measured data. In most parts of its validity range the accuracy is significantly improved compared to previous equations.

Keywords Aqueous solution · Correlation · Lithium bromide · Saline solution · Viscosity

1 Introduction

The extension of the operation range of absorption heat pumps and chillers with aqueous lithium bromide as working pair to evaporator temperatures below $0\text{ }^{\circ}\text{C}$ requires an additive in the refrigerant circuit to avoid freezing. Lithium Bromide (LiBr) is an obvious choice for this purpose. Thus, the need to calculate thermodynamic and transport processes as well as the need to evaluate measured data over an extended range of mass fraction and temperature arises. This depends on reliable and consistent property data.

The dynamic viscosity is an important measure for all calculations of heat and mass transfer related to flow phenomena. Ideally, a single correlation should be usable to accurately calculate viscosity from very dilute conditions near to pure water at temperatures below $0\text{ }^{\circ}\text{C}$ to concentrated solutions at high temperatures, to avoid inconsistencies. No currently available empirical or theoretical equation is able to provide this range.

✉ Christian Fleßner
christian.flessner@tu-berlin.de

Felix Ziegler
felix.ziegler@tu-berlin.de

¹ Institut für Energietechnik, Technische Universität Berlin, Marchstr. 18, 10587 Berlin, Germany

Fleßner et al. [1] presented an approach for a correlation of low-temperature thermophysical property data of dilute aqueous solutions of lithium bromide based on the experimental data of Sawada et al. [2] normalized with pure water properties calculated by IAPWS SR06-08 [3, 4]. The issue with the selected approach is its limitation to the low concentration range of the data it is based on. The correlation is not suitable for extrapolation to mass fractions higher than $\xi = 0.2$. Attempts to fit data over a wider range with the same form of correlation failed to deliver satisfactory results.

Simple theory-based approaches like the Falkenhagen [5] and Jones–Dole equations [6] are limited to very dilute solutions. Extensions like the semi-empirical Kaminsky equation [7] suffer from difficulties for the determination of the temperature dependence of their higher order coefficients. More recent approaches for a theoretical derivation like from Jiang and Sandler [8] are computationally too demanding for general purpose engineering calculations.

The often used correlation of Lee et al. [9] featured in the textbook by Herold et al. [10] is primarily centered on the mass fraction and temperature range encountered in absorber and desorber of absorption heat pumps, claiming a validity of $\xi = 0.45$ to 0.65 and $T = 312.9$ K to 427.7 K. The correlation used in the second edition of the same textbook [11] does not give any validity range at all. It is not published and available only via the help files of the calculation software EES [12].

The correlation of Kim and Infante Ferreira [13, p. 32] is based on the experimental data of Lee et al. [9] and unspecified data for pure water. A validity of $\xi = 0$ to 0.65 and 0°C to 220°C is claimed. A commercial implementation for several computational software suites [14] also exists.

To remedy the lack of an applicable equation ranging from below 0°C to high desorber temperatures, a simple new correlation extended from the form of [1] to fit the experimental data in a temperature range from -20°C to 110°C and from pure water to saline mass fractions of $\xi = 0.65$ is proposed. The limits of the temperature range are determined by the validity limits of the correlation chosen for the normalization [3]. In the present article, the data considered for this equation are analyzed first. In a next step the equation's form is derived from the experimental data's slope and suitable parameters are fitted. Finally, the correlation is compared to the experimental data with an additional comparison of existing correlations with the same set of data.

2 Analysis of Data

The experimental data of [2, 9, 15–23] have been compiled. Only measured data are used. Therefore, interpolated data like [24, 25] as well as the smoothed data reported in [16] have been excluded from the compilation of data. The data of Valyashko's compilation [26] were not used, since apart from the data of Lee et al. [9] it contains only data for temperatures outside the scope of this study (446 K and above). The data were collected either by extracting them from diagrams with WebPlotDigitizer [27] or by transcribing tabular data. Different units for salt content were converted to mass fraction. Temperature and dynamic viscosity were converted to K and Pa s.

The data sources with their respective limits and number of overall and excluded data points as well as the symbols used in Figs. 1, 2, 3, 4, 5, 6, 7, 8, 9, 10 are listed in Table 1.

The viscosity of pure water η_W used to determine the reduced viscosity (viscosity of solution divided by viscosity of solvent — η_{sol}/η_W) is calculated with IAPWS SR6-08 [3, 4] since it provides an accurate and computationally efficient equation with only temperature as the independent variable. Pressure dependence of thermophysical properties of aqueous solutions is not an issue at the moderate pressures encountered in absorption chillers and heat pumps (see the comparison in Appendix A). This correlation is valid from -20°C to 110°C , determining the limits of the presented correlation in terms of temperature. This range is sufficient for single-effect absorption heat pumps and chillers. For a further extension of validity aiming at multi effect chillers and heat pumps as well as heat transformers a different equation for pure water has to be used.

The limits concerning mass fraction are derived from the desire for an extrapolation to pure water on the one hand and from the highest mass fraction of measured data available on the other hand.

The range of data considered is displayed in Fig. 1. The dashed lines indicate the selected temperature range. The other boundaries are given by the calculated crystallization lines [28] and the overall selected mass fraction range. No significant gaps in the considered range are visible. The measured values not included into the fit are marked in a lighter shade of gray. It is visible that only data of Lee et al. [9] are above the upper boundary. The only data below the selected temperature range are from Mashovets et al. [19]. It is noticeable that some of the data are below the calculated crystallization line. This includes the lowest temperature data of [19] as well as single data points of [2, 23]. It cannot be discerned whether this is due to uncertainties of the calculated crystallization line, due to uncertainties of the respective author's mass fraction measurement or due to subcooled states in the experimental investigations. Since these data are still plausible within the usual uncertainty they were included into the correlation's database. Apart from data outside the desired validity range, further data points were excluded from the database before fitting. The data for pure water from Cao et al. [15] and Löwer [17] were not used, to avoid contradictions with the calculated pure water properties according to IAPWS SR6-08 [3] in the fitting process. Data points with a viscosity lower than that of pure water occurring in the datasets of Rohman et al. [21] and Sawada et al. [2] are also excluded from the fit. Though such a behavior occurs in some saline solutions like potassium bromide (see Jiang & Sandler [8]), all known experimental data or theoretical studies for lithium bromide apart from [21] and some data points of [2] show a monotonic increase of reduced viscosity with increasing salt content. Therefore, the respective data are discarded as unphysical.

Figure 2 shows the viscosity of all selected data points over T and ξ . Despite the high density of data points basic outlines of isosteric and isothermal lines are visible following the experimental conditions selected by their original authors. In Fig. 2a the viscosity of pure water is visualized with a dotted line with additional larger dots. Otherwise only the respective data's sources are distinguished with different

Table 1 Overview on data sources

Data source	T_{\min} (K)	T_{\max} (K)	ξ_{\min}	ξ_{\max}	n_{data}	n_{excl}	Symbol
Cao et al. [15]	303.15	343.15	0	0.5468	40	5 ^b	+
Hasaba et al. [16]	273.15	363.15	0.1143	0.6068	61	0	□
Lee et al. [9]	312.9	472.9	0.45	0.65	52	30 ^a	◇
Löwer [17]	273.15	373.15	0	0.65	147	11 ^b	○
Lo Surdo et al. [18]	278.15	338.15	0.0799	0.4648	33	0	▽
Mashovets et al. [19]	213.15	363.15	0.0506	0.4988	54	9 ^a	◁
Raatschen [20]	293.15	333.15	0.3	0.55	9	0	▷
Rohman et al. [21]	273.15	323.15	0.0105	0.5498	176	33 ^c	☆
Satoh et al. [22]	300.15	300.15	0.0502	0.3196	10	0	⊠
Sawada et al. [2]	264.57	298.69	0.05	0.2	74	7 ^c	×
Wimby et al. [23]	298.06	373.26	0.1531	0.5850	29	0	△

^aData outside the selected validity range are excluded from the correlation's database and are not included in Figs. 2, 3, 4, 5, 6, 7, 8, and 9

^bThe pure water data were not included into the correlation's database, but are included in Figs. 2, 3, 4, and 6

^cThe data below the viscosity of pure water were removed from the correlation's database, see below. They are still included in Figs. 2, 3, 4, and 6

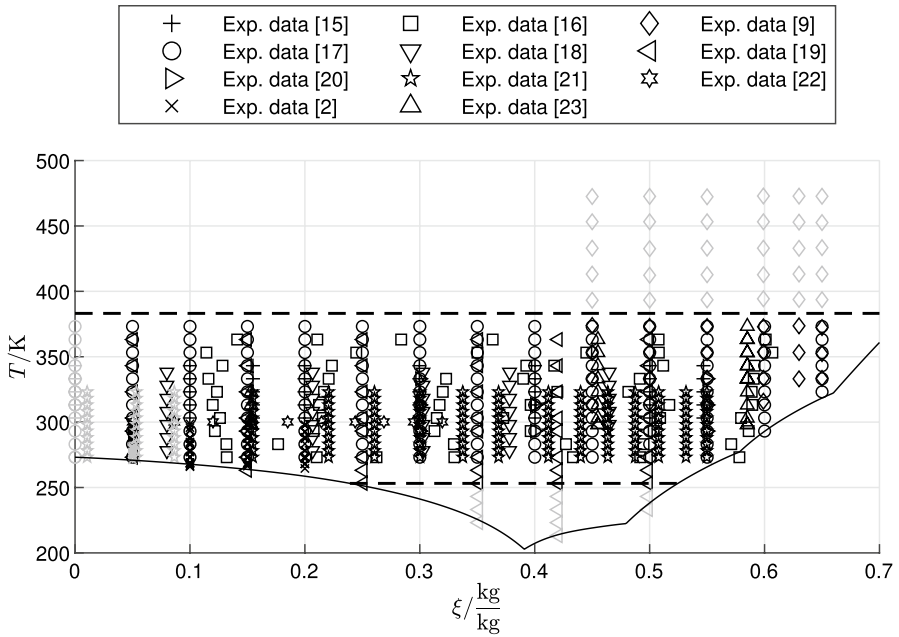


Fig. 1 Crystallization line and measured data used for correlation, Symbols for data sources in the legend according to Table 1

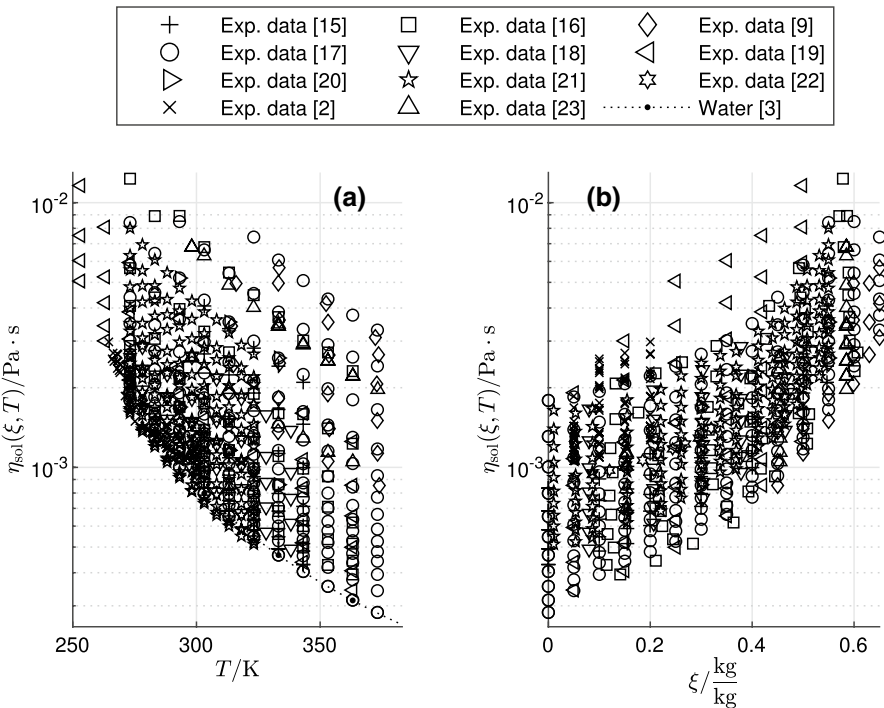


Fig. 2 Viscosity over T (a) and ξ (b), measured data, not filtered, Symbols for data sources in the legend according to Table 1

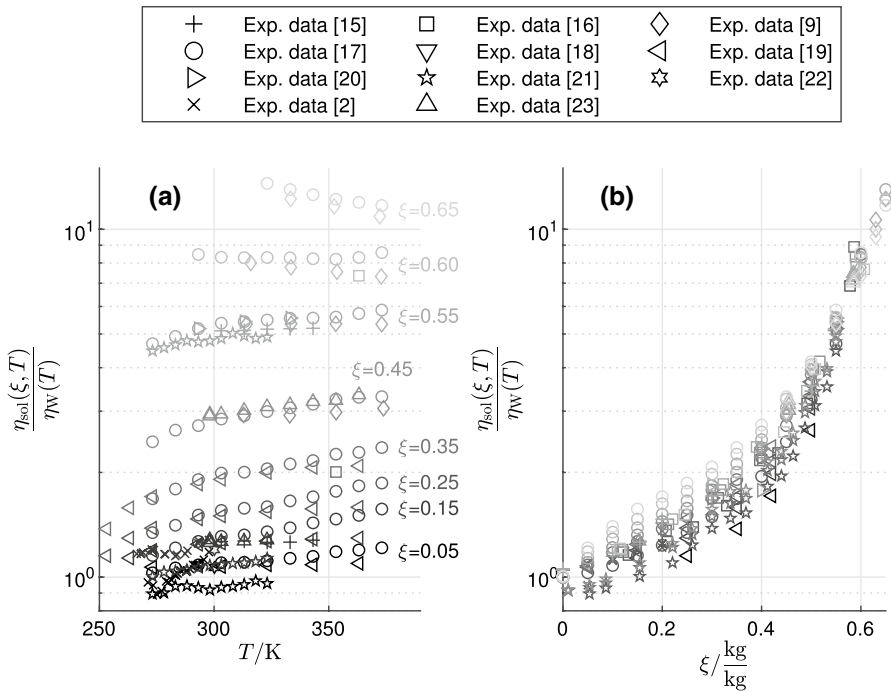


Fig. 3 Reduced viscosity over T (a) and ξ (b), experimental data filtered along isosteric and isothermal lines, Symbols for data sources in the legend according to Table 1

symbols. The general trend shows a decrease of viscosity with increasing temperature and an increase of viscosity with increasing mass fraction.

To distinguish the influence of ionic interaction from water/water interactions the reduced viscosity $\eta_{\text{sol}}/\eta_{\text{W}}$ is plotted in Fig. 3 over temperature and mass fraction. To enable a more detailed discussion of the data's relationship to temperature and concentration the data were filtered in terms of isosteric and isothermal groups with a tolerance of $\Delta\xi = \pm 0.005$ along the isosteric lines and a tolerance of $\Delta T = \pm 1$ K along the isothermal lines. The number of values included into each group and the exact parameters for the respective datasets are shown in Table 2 for the isosteric groups and in Table 3 for the isothermal groups. In Table 3 the minimum and maximum temperatures reported in the original sources are given if applicable. Otherwise the single value reported is given.

The distinction between the different sources is identical to Fig. 2. Additionally, data grouped along the isosteric and isothermal lines are distinguished by different grayscales. Generally, the agreement of the different datasets is satisfactory. The data of Rohman et al. [21] are an exception. At all isosteric groups but especially at mass fractions below $\xi = 0.2$ reduced viscosities of [21] are significantly below the other source's data. For all values in the $\xi = 0.05$ isosteric group, the reduced viscosity is slightly smaller than 1, indicating a lower viscosity than pure water. As stated above, this contradicts all known other experimental and theoretical studies, reducing the respective measurement's credibility.

Table 2 Experimental data assigned to isosteric groups for Fig. 3a with nominal ξ

Data source	0.05		0.15		0.25		0.35		0.45		0.55		0.6		0.65	
	n	ξ	n	ξ	n	ξ	n	ξ	n	ξ	n	ξ	n	ξ	n	ξ
Cao et al. [15]	0	N.A.	5	0.1548	0	N.A.	0	N.A.	0	N.A.	5	0.5468	0	N.A.	0	N.A.
Hasaba et al. [16]	0	N.A.	0	N.A.	0	N.A.	1	0.3502	0	N.A.	0	N.A.	1	0.601	0	N.A.
Lee et al. [9]	0	N.A.	0	N.A.	0	N.A.	0	N.A.	4	0.45	4	0.55	4	0.599	3	0.65
Löwer [17]	11	0.05	11	0.15	11	0.25	11	0.35	11	0.45	11	0.55	9	0.6	6	0.65
Lo Surdo et al. [18]	0	N.A.	0	N.A.	0	N.A.	0	N.A.	0	N.A.	0	N.A.	0	N.A.	0	N.A.
Mashovets et al. [19]	6	0.0506	7	0.1499	8	0.2506	8	0.3501	0	N.A.	0	N.A.	0	N.A.	0	N.A.
Raatschen [20]	0	N.A.	0	N.A.	0	N.A.	0	N.A.	0	N.A.	0	N.A.	3	0.55	0	N.A.
Rohman et al. [21]	11	0.0534	11	0.1545	0	N.A.	0	N.A.	0	N.A.	0	N.A.	11	0.5498	0	N.A.
Satoh et al. [22]	1	0.0502	1	0.1530	0	N.A.	0	N.A.	0	N.A.	0	N.A.	0	N.A.	0	N.A.
Sawada et al. [2]	21	0.05	16	0.15	0	N.A.	0	N.A.	0	N.A.	0	N.A.	0	N.A.	0	N.A.
Wimby et al. [23]	0	N.A.	5	0.1531	0	N.A.	0	N.A.	0	N.A.	0	N.A.	0	N.A.	0	N.A.

Table 3 Experimental data assigned to isothermal groups for Fig. 3b with nominal T

Data source	253.15 K		263.15 K		273.15 K		293.15 K		313.15 K		333.15 K		353.15 K		373.15 K	
	n	T/K	n	T/K	n	T/K	n	T/K	n	T/K	n	T/K	n	T/K	n	T/K
[15]	0	N.A.	0	N.A.	0	N.A.	0	N.A.	8	313.15	8	333.15	0	N.A.	0	N.A.
[16]	0	N.A.	0	N.A.	7	273.15	6	293.15	6	313.15	6	333.15	6	353.15	0	N.A.
[9]	0	N.A.	0	N.A.	0	N.A.	0	N.A.	1	312.9	6	333.00	4	353.10	4	372.90
[17]	0	N.A.	0	N.A.	12	273.15	13	293.15	13	313.15	14	333.15	14	353.15	14	373.15
[18]	0	N.A.	0	N.A.	0	N.A.	0	N.A.	0	N.A.	0	N.A.	0	N.A.	0	N.A.
[19]	4	253.15	5	263.15	6	273.15	6	293.15	0	N.A.	0	N.A.	0	N.A.	0	N.A.
[20]	0	N.A.	0	N.A.	0	N.A.	3	293.15	4	313.15	0	333.15	2	353.15	0	N.A.
[21]	0	N.A.	0	N.A.	16	273.15	16	293.15	16	313.15	0	N.A.	0	N.A.	0	N.A.
[22]	0	N.A.	0	N.A.	0	N.A.	0	N.A.	0	N.A.	0	N.A.	0	N.A.	0	N.A.
[2]	0	N.A.	0	N.A.	9	272.79	6	292.85	0	N.A.	0	N.A.	0	N.A.	0	N.A.
						273.42	293.40									
[23]	0	N.A.	0	N.A.	0	N.A.	0	N.A.	3	313.07	4	333.08	3	353.13	1	373.26
										313.09		333.17		353.17		

Overall the temperature dependence of reduced viscosity is small, as visible in the shallow gradients in Fig. 3a as well as in the dense stacking of isothermal lines in Fig. 3b. Therefore, temperature dependence of viscosity is induced primarily by the temperature dependence of water/water interaction. For mass fractions up to $\xi = 0.55$ the reduced viscosity increases with rising temperature (Fig. 3a). The gradient with respect to temperature decreases with increasing mass fraction. At $\xi = 0.6$ the data of Löwer [17] on the one hand and the data of Hasaba et al. [16] and Lee et al. [9] on the other hand are divergent at temperatures above 350 K, resulting in different gradients with respect to temperature. In the isosteric group for $\xi = 0.65$ the slope is clearly inverted. This inversion between $\xi = 0.55$ and 0.65 roughly coincides with the peritectic point at $\xi = 0.5781$ between the solid states of LiBr–3H₂O and LiBr–2H₂O [28]. Since the data's resolution in terms of mass fraction in this range is limited, it is not possible to exactly determine the point of inversion from the experimental data, but the change of crystalline hydrate structure may be a physical reason.

The change of gradient concerning temperature and its later inversion is also visible in subfigure (b) in the crossing over of the isothermal groups between $\xi = 0.55$ and 0.65. Obviously, the dependence of reduced viscosity on mass fraction increases with increasing mass fraction, while the influence of temperature on the mass fraction dependence is overall small.

3 Correlation Method

The basic approach for data correlation of the previous publication [1] was an empirical equation for the reduced viscosity $\eta_{\text{sol}}/\eta_{\text{W}}$ with exponents as fit parameters (Eq. 1). Absolute temperature T is divided by the critical temperature $T_{\text{crit}} = 647.096$ K [29] to avoid differences of magnitude between the independent variables.

$$\frac{\eta_{\text{sol}}}{\eta_{\text{W}}} = 1 + a \cdot \left(\frac{T}{T_{\text{crit}}} \right)^b \cdot \xi^c. \quad (1)$$

The new approach for correlating the aggregated experimental data is derived from Eq. 1. Two modifications are made from Eqs. 1 to 2. Firstly, the equation was changed to a logarithmic form to better account for the small changes of reduced viscosity at low salt content as well as the increasing sensitivity to mass fraction at higher salt content. Secondly, the exponent b of the reduced temperature T/T_{crit} in (1) was expanded to a linear mass fraction dependence with the independent arbitrary coefficients b_1 and b_2 as an empirical first order approximation of the inverted gradient in respect of temperature at mass fractions above $\xi = 0.55$.

$$\ln \left(\frac{\eta_{\text{sol}}}{\eta_{\text{W}}} \right) = a \cdot \left(\frac{T}{T_{\text{crit}}} \right)^{(b_1 + b_2 \cdot \xi)} \cdot \xi^c. \quad (2)$$

In addition to the new features, Eq. 2 basically satisfies the same requirements as the previous one. For $\xi = 0$ it converges to the viscosity of pure water and the basic behavior is qualitatively consistent with the physical constraints even outside of its designated validity.

For the fitting process, available data were first aggregated and prepared. Data points for pure water and for temperatures and mass fractions outside of the desired range of validity were removed. Then reduced viscosities were calculated from the saline solution's measured viscosity data and the related calculated viscosity of pure water. In the next step data points with $(\eta_{\text{sol}}/\eta_{\text{W}}) < 1$ were excluded from the dataset in accordance with the criteria defined in Sect. 2. The measured temperature values were normalized by division by the critical temperature of water T_{crit} [29].

The coefficients of Eq. 2 were fitted with MATLAB's curve fitting toolbox [30] with mass fraction ξ and normalized temperature (T/T_{crit}) as independent variables and the natural logarithm of reduced viscosity $\ln(\eta_{\text{sol}}/\eta_{\text{W}})$ as dependent variable. The coefficients to be fitted are a , b_1 , b_2 , and c . A least absolute deviations regression method (see [31]) (LAR in MATLAB-nomenclature) with a trust-region algorithm was used. This method is more robust in terms of outliers. Otherwise, no weighting and explicit outlier detection were applied. Solutions of the iteration of the regression problem may vary with different start values, so the fitting process was repeated 1.000 times with random start values. The goodness of fit was determined with the same parameters, automatically provided by MATLAB (see Field [32]), nomenclature from MATLAB), as in the previous article [1]. All parameters were additionally checked by separate calculation from Eqs. 3 to 7:

DFE The degree of freedom for errors, respectively, residuals (*DFE*) is the difference between the number of measured values the correlation is based on n and the number of estimated coefficients p , (Eq. 3). In the present article n is the sum of all measured values finally used for the correlation and the number of estimated coefficients p is 4. This parameter is reported in Sect. 4 to facilitate the assessment of other parameters.

$$DFE = n - p. \quad (3)$$

SSE/RMSE Despite using a least absolute deviations method, the final evaluation of goodness of fit is evaluated by a common sum of square method. The residual sum of squares or sum of squares estimate of errors (*SSE*) is the sum of squares of the difference between the observed data y_i and the value predicted by the model \hat{y}_i (Eq. 4). The root-mean-square deviation or error (*RMSE*) is the root of the quotient of this difference and the degree of freedom for residuals (see Eqs. 3 and 5). Both parameters have to be minimal. Only *RMSE* is reported in Sect. 4 because of the close relationship of both quantities.

$$SSE = \sum_{i=1}^n (y_i - \hat{y}_i)^2 \quad , \quad (4)$$

$$RMSE = \sqrt{\frac{\sum_{i=1}^n (y_i - \hat{y}_i)^2}{DFE}} \quad , \quad (5)$$

R^2/R^2_{adj} : The coefficient of determination R^2 quantifies the proportion of variance in the dependent variable that is predictable from the independent variables (Eq. 6). The adjusted coefficient of determination R^2_{adj} accounts for the degree of freedom for residuals (DFE) (Eq. 7). Since the quotient $((n - 1)/DFE)$ is close to one in the present case, this parameter deviates only slightly from the coefficient of determination. Therefore, only this value is reported in Sect. 4. Both parameters are optimal for a value of 1.

$$R^2 = 1 - \frac{\sum_{i=1}^n (y_i - \hat{y}_i)^2}{\sum_{i=1}^n (y_i - \bar{y}_i)^2} \quad , \quad (6)$$

$$R^2_{adj} = 1 - \frac{(n - 1)}{DFE} \cdot \frac{\sum_{i=1}^n (y_i - \hat{y}_i)^2}{\sum_{i=1}^n (y_i - \bar{y}_i)^2} \quad . \quad (7)$$

The final set of fitted parameters was chosen by a minimum/maximum search within the stored goodness of fit parameters. The selected fit was optimal in all parameters evaluated.

4 Results

Table 4 lists the final estimated parameters for Eq. 2 as well as the absolute and relative 95 % confidence bounds. The narrow relative confidence bounds indicate a high significance of the chosen parameters. The parameter c in Eq. 2 has a significantly wider 95 % confidence interval than the other parameters. This is mainly due to the mass fraction appearing also in the exponent of T/T_{crit} in conjunction with the parameter b_2 . Therefore the impact of this parameter on the fit’s accuracy is smaller, but still relevant. Leaving it out would have a significantly negative impact on the goodness of fit.

Table 4 Parameters for Eq. 2

	a	b_1	b_2	c
Estimated parameter	2.477	3.609	− 5.871	0.2365
95 % confidence bound absolute	± 0.207	± 0.168	± 0.329	± 0.0913
95 % confidence bound relative	± 8.4 %	± 4.7 %	± 5.6 %	± 38.6 %

Table 5 Goodness of fit parameters

	<i>n</i>	<i>p</i>	<i>DFE</i>	<i>RMSE</i>	<i>R</i> ² _{adj}
Present correlation (Eq. 2)	586	4	582	0.06822	0.9885
Previous correlation [1]	98	3	95	0.04711	0.9969
Lee et al. [9]	162	9	153	0.07816	0.9924
SSC (EES) [12]	586	9	577	0.15655	0.9393
Kim and Infante Ferreira [13]	563	16	547	0.08554	0.9817

The goodness of fit parameters are listed in Table 5. For comparison the respective parameters for the present author’s previous model [1], Lee et al. [9], the SSC-correlation used in EES [12], and Kim and Infante Ferreira [13] are listed each for the section of the compiled experimental data within the selected correlation’s respective limits of validity. The limits for the SSC-Correlation [12] are not known, therefore it is applied to all aggregated data.

The goodness of fit parameters reported in Table 5 show that the present correlation compares favorably with the other equations benchmarked against the same set of data or fractions thereof. Additionally the presented equation covers its range of validity with a comparatively small number of fitted coefficients.

To enable comparison of implementations of the new correlation, Table 6 lists calculated values for the viscosity of water η_W and solution $\eta_{sol}(T, \xi)$ for different temperatures and mass fractions calculated with Eq. 2. The numbers are rounded to 6 significant digits.

4.1 Comparison with Experimental Data

Figure 3 shows viscosity over temperature (a) and mass fraction (b). The experimental data points are the same as used in Fig. 3. Additionally, the viscosity for pure water according to [3] and the isosteric and isothermal lines according to Eq. 2 are plotted within the validity limits of the correlation indicated by temperature and mass fraction and the crystallization limits calculated according to [28].

The agreement of experimental data and the calculated isolines in Fig. 4 are very good. The general trend of the experimental data is well reproduced by the calculated isosteric and isothermal lines and the absolute deviations are small. The data of Rohman et al. [21] display a systematic deviation to lower values at low mass

Table 6 Calculated values of viscosity

	253.15 K	273.16 K	293.15 K	333.15 K	383.15 K
$\eta_W = \eta_{sol}(T, \xi = 0)/\text{mPa s}$	4.39176 ^a	1.79116	1.00157	0.466039	0.254591 ^b
$\eta_{sol}(T, \xi = 0.2)/\text{mPa s}$	5.21742	2.20382	1.28120	0.652277	0.408389
$\eta_{sol}(T, \xi = 0.4)/\text{mPa s}$	8.09039	3.50890	2.08886	1.10537	0.713234
$\eta_{sol}(T, \xi = 0.6)/\text{mPa s}$	–	–	7.77985	3.70345	2.07477

^aMetastable state (subcooled liquid)

^bMetastable state (superheated liquid)

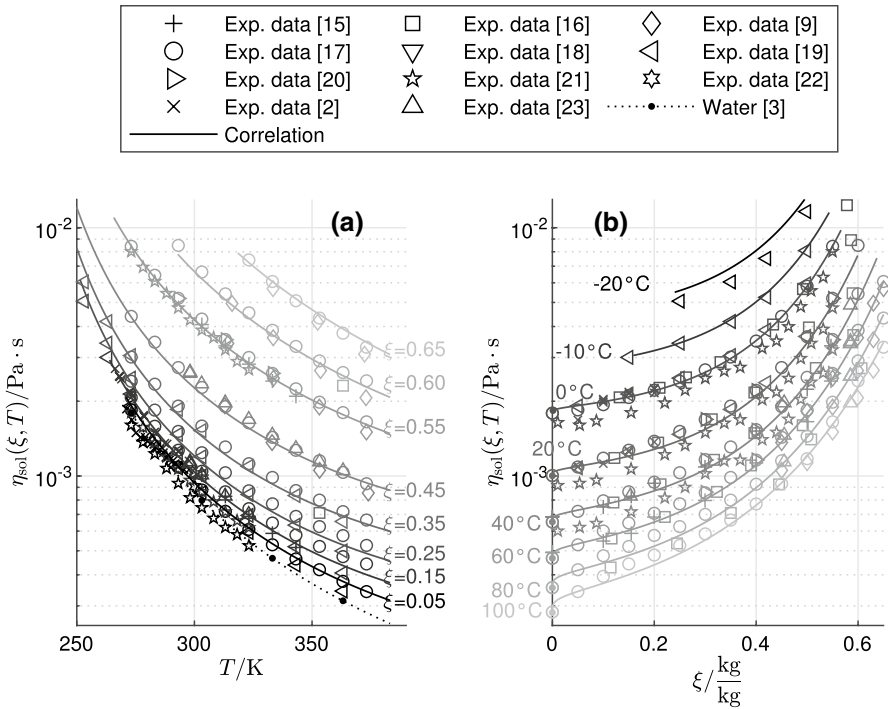


Fig. 4 Viscosity over T (a) and ξ (b), experimental data filtered along isosteric and isothermal lines with calculated lines from Eq. 2, Symbols for data sources in the legend according to Table 1

fractions visible especially in Fig. 4b. This deviation is visible in respect to the correlation as well as to all other experimental data compiled here. The predicted viscosity for -20°C is above the measured data by Mashovets et al. [19] for all mass fractions displayed. For all other sources no systematic bias is visible in Fig. 4.

The relative deviation of the fitted viscosity to the experimental data is plotted in Fig. 5. The data plotted in this diagram comprise all data that were used for fitting. Data points excluded from the fit-like data for pure water by Cao et al. [15] and Löewer [17] or the data with a reduced viscosity ($\eta_{\text{sol}}/\eta_{\text{W}} < 1$) from Rohman et al. [21] and Sawada et al. [2] are not considered in this comparison. The correlation deviates no more than $\pm 10\%$ from most experimental data, which is deemed acceptable, since the measured data are highly scattered in itself. Concerning the data of Rohman et al. [21] the correlation always overpredicts the experimental data up to $+19\%$. Since the measured viscosities of Rohman et al. are significantly lower than all other sources data, this is not critical. The correlation's deviation from the lowest temperature data of Mashovets et al. [19] is between $+10\%$ and $+17\%$ as already visible in Fig. 4. Since no other data are available for comparison and the experimental uncertainty of this specific data series is unknown, the consequences of this deviation remain unclear. For some data points of Hasaba et al. [16] and a single data point of Raatschen [20] the correlation deviates up to -25% and $+26\%$, respectively. As these data deviate from

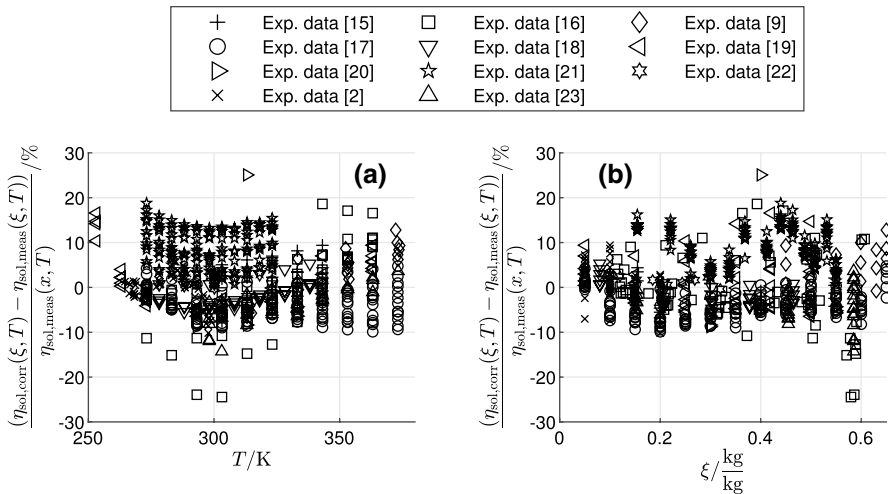


Fig. 5 Relative deviation of calculated from measured data over (a) T and ξ (b). Symbols for data sources in the legend according to Table 1

most other experimental data, this divergence does not challenge the correlation's credibility.

4.2 Comparison with Other Correlations

In Fig. 6 the viscosity calculated by Eq. 2 as well as the previous correlation [1], Lee et al. [9], the SSC-Correlation [12], and Kim and Infante Ferreira [13] are compared with experimental data in respect to temperature and mass fraction. To improve clarity, less data and isosteric and isothermal lines are used than in previous plots.

In Fig. 6 the limits of the correlations from literature are easily discernible. While Eq. 2 captures the slope in relation to temperature as well as in relation to mass fraction, the previous correlation [1] (indicated with dash-dotted lines) diverges from the data outside of its validity range with the isosteric lines for $\xi = 0.45$ and 0.65 bearing no relation to the experimental data at all and the predicted line for $\xi = 0.25$ diverging from the experimental data for temperatures higher than 300 K. In Fig. 6b the isothermal lines for -20°C and 20°C are deviating from the measured data above $\xi = 0.25$, while the calculated viscosity for 60°C and 100°C exhibits a completely different behavior concerning curvature and absolute values than the experimental data.

The correlation of Lee et al. [9] (indicated with dotted lines) exhibits a similar behavior with even stronger divergence from the experimental data in respect to mass fraction. For 60°C and 100°C the calculated line follows the experimental data closely down to $\xi \approx 0.25$. For lower mass fractions a minimum of viscosity is reached, with a steep increase toward $\xi = 0$, completely missing the experimental data for low mass fractions. At 20°C and -20°C this departure occurs near $\xi = 0.4$.

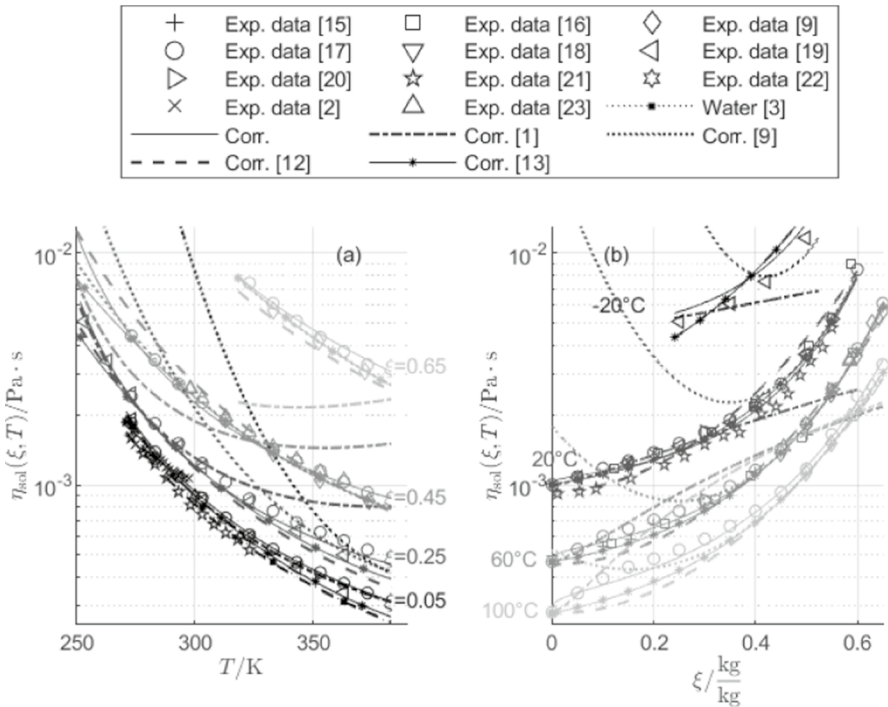


Fig. 6 Viscosity over T (a) and ξ (b), experimental data filtered along isosteric and isothermal lines with isolines from Eq. 2 as well as from [1, 9, 12], Symbols for data sources in the legend according to Table 1

So both correlations with a stated limited range of validity [1, 9] are well suited to predict viscosity data within their respective limits. However, an extrapolation is not possible in both cases, leaving a significant gap between the maximum mass fraction of [1] $\xi = 0.20$ and the minimum mass fraction of [9] $\xi = 0.45$.

The SSC-Correlation [12] (indicated with dashed lines) has no stated range of validity. Its dependence on temperature as visible in Fig. 6a reasonably mirrors the experimental data. The isosteric lines for $\xi = 0.05$ and 0.25 diverge visibly from the experimental data above $T \approx 320$ K. For $\xi = 0.05$ the calculated viscosity for aqueous LiBr solution is nearly identical to the water line calculated by [3]. The plot with respect to mass fraction Fig. 6b reveals a systematic deviation from most experimental data for mass fractions below $\xi \approx 0.4$, with a predicted viscosity for pure water slightly below that calculated with [3]. Therefore, the newest correlation from the previous state of the art featured in textbooks fares qualitatively well in predicting the viscosity of aqueous LiBr solution but displays systematic divergence in detail.

The correlation of Kim and Infante Ferreira [13] (solid line with additional stars) follows the experimental data closely. In Fig. 6 below $\xi = 0.4$, in a range where the underlying data of Lee et al. [9] offer no data, a slight diversion from the measured data for the isothermal groups at 60°C and 100°C is visible. This correlation

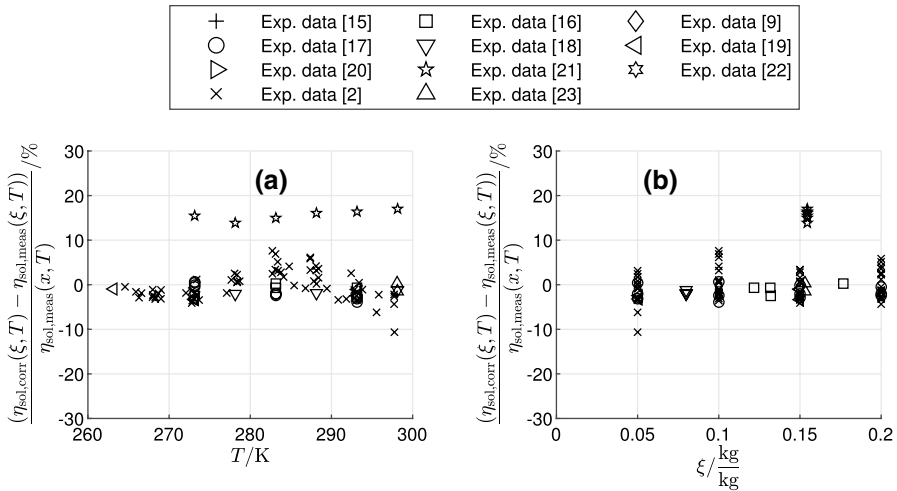


Fig. 7 Relative deviation of calculated from measured data over T (a) and ξ (b), previous correlation [1], Symbols for data sources in the legend according to Table 1

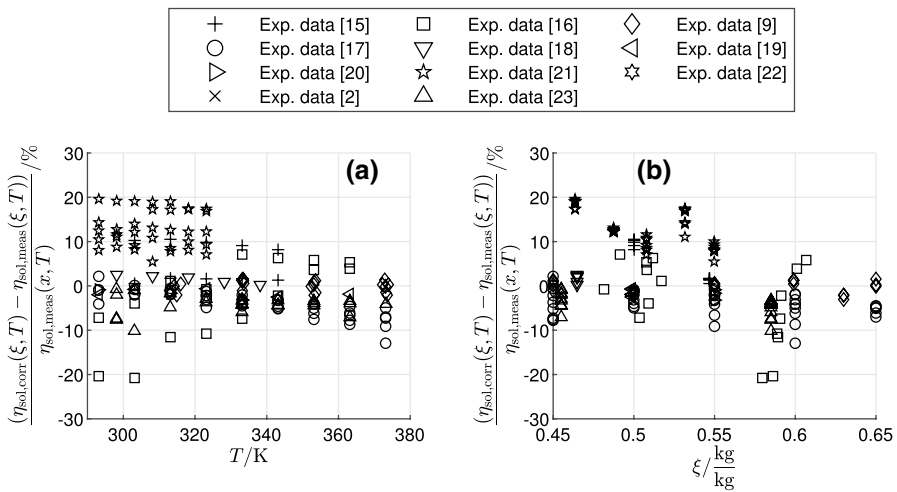


Fig. 8 Relative deviation of calculated from measured data over T (a) and ξ (b), equation of Lee et al. [9], Symbols for data sources in the legend according to Table 1

is within a reasonable range compared with the data of Mashovets et al. [30] for the isothermal group at -20°C with less systematic bias than Eq. 2. Overall, the correlation of Kim and Infante Ferreira [13] is successful in predicting viscosity according to measured data from literature within the range defined for the present correlation.

To get a deeper impression of the accuracy of the new correlation compared with previous ones, plots for the relative deviation of [1] (Fig. 7), [9] (Fig 8), [12] (Fig. 9) and [13] (Fig. 10) are discussed in comparison with Fig. 5. The goodness of fit parameters

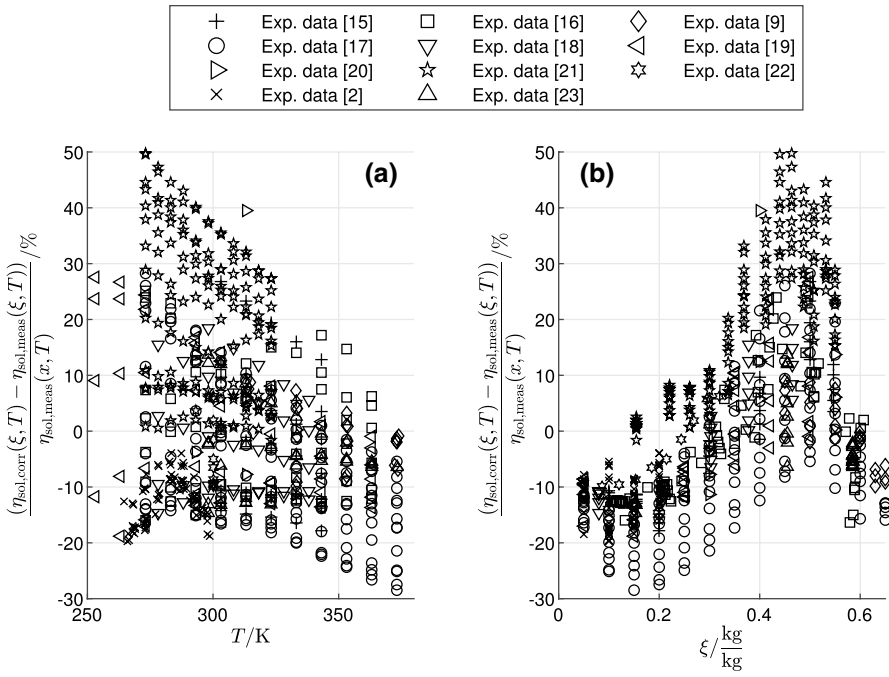


Fig. 9 Relative deviation of calculated from measured data over T (a) and ξ (b), SSC-correlation from EES [12], Symbols for data sources in the legend according to Table 1

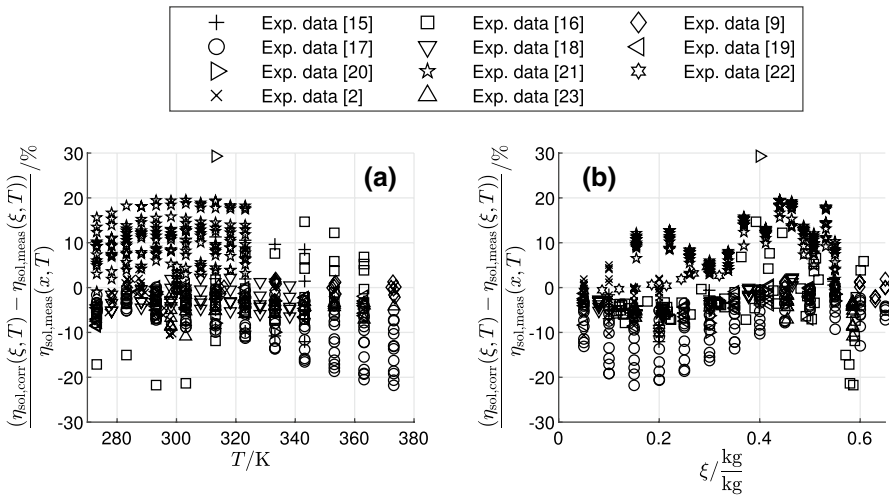


Fig. 10 Relative deviation of calculated from measured data over T (a) and ξ (b), Equation of Kim and Infante Ferreira [13], Symbols for data sources in the legend according to Table 1

are already been presented in Table 5, showing no significant differences in goodness of fit between the different correlations. For the comparison the aggregated experimental data within the claimed validity of the respective correlation are considered. The data points excluded from the fit for various reasons are not plotted, as in Fig. 5.

The relative deviation of the previous correlation [1] to the experimental data shown in Fig. 7 is almost completely within the $\pm 10\%$ range with most of the data within the $\pm 5\%$ range. Only one data series of Rohman et al. [21] for a mass fraction of $\xi = 0.1545$ (vertical stack of pentagrams in Fig. 7b) is within the validity range of this correlation. The correlation predicts up to 17% larger viscosities than reported in [21]. Again, the general deviation of these data from other experimental data at similar conditions reduces its relevance for the comparison. Within its narrow range of validity the previous correlation is more precise than Eq. 2, but it is not suitable for the extended range of data as can be deduced from the extrapolation behavior visible in Fig. 6.

Similarly, the correlation of Lee et al. [9] works well within its defined range of validity, as can be seen in Fig. 8 with a relative deviation roughly equal to the presented correlation, Eq. 2 as presented in Fig. 5, i.e., mostly within the $\pm 10\%$ range. For some data of Hasaba et al. [16] and most data of Rohman et al. the correlation deviates up to $\pm 20\%$ from the experimental data. The extrapolation of the data to lower mass fractions is impossible as already shown in the discussion of Fig. 6.

The SSC-Correlation [12] follows the experimental data in Fig. 6 qualitatively well with some noticeable systematic deviations. Figure 9 reveals the amount of relative deviation. Even if the measured data of Rohman et al. [21] were to be discarded, the relative deviation is spread in a $\pm 30\%$ interval. For high temperatures as well as for low mass fractions the correlation predicts values lower than the experimental data. For low temperatures as well as for most high mass fraction data the calculated results are higher than the experimental data. Since correlation's underlying data as well as its desired validity is unknown, no range where this correlation is safely usable can be determined.

The deviation of the correlation of Kim and Infante Ferreira [13] from the measured data is plotted in Fig. 10. Overall the range of deviation is similar to the new correlation shown in Fig. 5. As for all correlations, the data of Rohman et al. [21] are not captured well, with maximum deviations of +20%. Again, this is uncritical since the data of Rohman et al. diverge from the general trend of experimental data. The correlation deviates from the outlying data of Hasaba et al. [16] and Raatschen [20] by up to -21% and $+29\%$, respectively. Furthermore the correlation exhibits a deviation from the data of Löwer [17] up to -22% for high temperatures and low mass fractions which are not covered by the measured data of Lee et al. [9] on which the correlation [13] is based on. Overall, the correlation of Kim and Infante Ferreira [13] has a similar but slightly larger deviation from measured data than the proposed correlation (Eq. 2).

5 Conclusion

The presented simple empirical correlation is able to calculate viscosity data over a range sufficient for dilute solutions in low-temperature evaporators with LiBr as anti-freeze agent to concentrated solutions at high desorber temperatures in single-effect absorption heat pumps and chillers. The correlation's accuracy is nearly

equal or even better than existing correlations, even those intended for a more limited range of validity. The new correlation fares actually better than the most recent equation by Kim and Infante Ferreira [13] due to the broader base of experimental data. The form of the proposed correlation is advantageous compared with the other approaches since the desired accuracy is reached with only 4 coefficients compared with 9 coefficients for [9, 12] or 16 coefficients for [13]. For temperatures above 110 °C a different equation for the viscosity of pure water is necessary to apply the chosen approach to the existing experimental data. While this is out of scope for the present work, it is a promising approach, provided a pure water equation simple enough not to compromise computation time can be found. Since the measured data are highly scattered especially in the dilute region at low temperature, additional high-quality data for the range below $\xi = 0.3$ and $T = 273$ K are desirable.

Appendix A: Pressure Influence on Reference Viscosity

The correlation used for the reference viscosity of pure water IAPWS SR06-08 [3, 4] does not consider pressure variation. In this appendix it is compared with IAPWS R12-08 [33, 34], in order to investigate the influence of saturation pressure variation in relation to the desired temperature range. The liquid density necessary for IAPWS R12-08 was calculated iteratively in dependence on temperature and pressure with the IAPWS 95 formulation [35, 36] with the MATLAB implementation of Junglas [37]. For the subcooled metastable region IAPWS R12-08 is declared to be "(...) in fair agreement (within 5 %) with available data down to 250 K" [33]. The IAPWS 95 release is claimed to "behave reasonably" [35] when extrapolated into the metastable regions for subcooled as well as for superheated liquid.

The minimum pressure p_{\min} encountered in the system and temperature range considered is the saturation pressure at -20 °C and the corresponding crystallization mass fraction of $\xi = 0.5246$ [28]. It is estimated by extrapolating the correlation of Kim and Infante Ferreira [38]. Though the uncertainty of this estimation is unknown, the magnitude is appropriate. The highest pressure p_{\max} that can be sensibly assumed is the saturation pressure of pure water at 110 °C calculated with IAPWS 95. Pressures are listed in Table 7 alongside the densities and viscosities calculated with both correlations at the extremal values of temperature and pressure.

Table 7 Comparison of pure water data calculated by different calculations

Correlation	p/kPa	-20 °C		110 °C	
		$\rho/\text{kg} \cdot \text{m}^{-3}$	$\eta_{\text{w}}/\text{Pa s}$	$\rho/\text{kg} \cdot \text{m}^{-3}$	$\eta_{\text{w}}/\text{Pa s}$
IAPWS SR06-08 [3]	100 ^a	993.6	0.004392	950.9	2.546×10^{-04}
IAPWS 95 [35]/R12-08 [33]	0.02054 ^b	993.5	0.004394	950.9	2.546×10^{-04}
	143.4 ^c	993.6	0.004391	950.9	2.546×10^{-04}

^aPressure fixed by correlation's definition

^bCalculated by [38] for -20 °C and $\xi = 0.5246$.

^cCalculated by [35, 37] for 110 °C

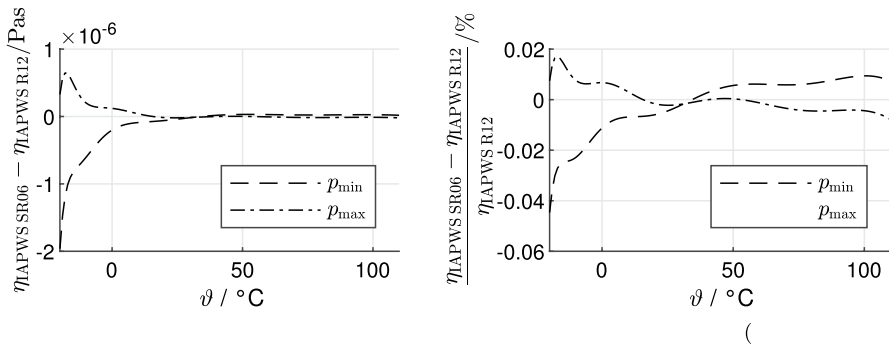


Fig. 11 Absolute and relative deviation of calculated pure water viscosity (IAPWS SR06-08 from IAPWS R12-08) for different pressures

It is easily discernible that the range of pressure considered has little effect on viscosity. For an impression over the full temperature range, the absolute and relative deviations of SR06-08 from R12-08 at p_{\min} and p_{\max} are plotted in Fig. 11. Absolute and relative deviation are far below the usual experimental uncertainty. Therefore, using the simplified correlation SR06-12 for the reference viscosity of pure water and neglecting the pressure dependence has no significant influence on the new correlation’s accuracy. The maximum deviation of -0.5% occurs in the subcooled region. This is still negligible compared with the experimental uncertainty of the data in that range.

Appendix B: Fit Options

Table 8 lists the modified fit options in MATLAB [30]. Otherwise the default settings were used. The modified settings were implemented either to reduce the influence of outliers (Robust setting) or to reliably reach convergence of the iteration (MaxFunEvals, MaxIter, TolFun, TolX).

Table 8 Modified fit options in MATLAB [30] for fitting Eq. 2

Parameter	Description	Default value	Value
Robust	Robust fitting method	‘Off’	‘LAR’
MaxFunEvals	Maximum number of evaluations of model	600	6000
MaxIter	Maximum number of iterations for fit	400	4000
TolFun	Termination tolerance on model value	10^{-6}	10^{-10}
TolX	Termination tolerance on coefficient values	10^{-6}	10^{-10}

Acknowledgements The authors wish to thank Dr. Niccolò Gianneti (Waseda University, Tokyo) for providing Japanese literature [16, 24] and Leonard Thraen (TU Berlin) for the translation of these articles.

Author Contributions The concept of the article was developed by CF. Data compilation, programming of fits, and the generation of figures were performed by CF. The mathematical form of the correlation was developed by CF with refinement in discussion with FZ. The first draft was written by CF with critical revision by FZ. All authors read and approved the final manuscript.

Funding Open Access funding enabled and organized by Projekt DEAL. The research for this article was funded by the German Federal Ministry for Economic Affairs and Climate Action within the joint project with Fraunhofer Institute for Solar Energy Systems ISE *Sorption evaporators for boiling temperatures below 0 °C—platform for scientific quality (SubSie-Plattform)* under Grant Number 03EN2012B.

Data Availability Compiled experimental data and MATLAB scripts as well as saved workspaces are available from the corresponding author upon reasonable request.

Declarations

Conflict of interest The authors have no relevant financial or non-financial interests to disclose.

Open Access This article is licensed under a Creative Commons Attribution 4.0 International License, which permits use, sharing, adaptation, distribution and reproduction in any medium or format, as long as you give appropriate credit to the original author(s) and the source, provide a link to the Creative Commons licence, and indicate if changes were made. The images or other third party material in this article are included in the article's Creative Commons licence, unless indicated otherwise in a credit line to the material. If material is not included in the article's Creative Commons licence and your intended use is not permitted by statutory regulation or exceeds the permitted use, you will need to obtain permission directly from the copyright holder. To view a copy of this licence, visit <http://creativecommons.org/licenses/by/4.0/>.

References

1. C. Fleßner, L. Thraen, F. Ziegler, Low-temperature correlation of property data for dilute aqueous lithium bromide solution. *Chem. Eng. Technol.* **44**, 1783–1791 (2021). <https://doi.org/10.1002/ceat.202100209>
2. I. Sawada, M. Yamada, S. Fukusako, T. Kawanami, Thermophysical properties of aqueous solutions near the equilibrium freezing temperature. *Int. J. Thermophys.* **19**, 749–759 (1998). <https://doi.org/10.1023/A:1022626503214>
3. IAPWS, Revised supplementary release on properties of liquid water at 0.1 MPa. Technical Report IAPWS SR6-08(2011) (The International Association for the Properties of Water and Steam, 2011), <http://www.iapws.org/relguide/LiquidWater.html>
4. J. Pátek, J. Hrubý, J. Klomfar, M. Součková, A.H. Harvey, Reference correlations for thermophysical properties of liquid water at 0.1 MPa. *J. Phys. Chem. Ref. Data* **38**, 21–29 (2009). <https://doi.org/10.1063/1.3043575>
5. H. Falkenhagen, M. Dole, Vorläufige Mitteilung. Das Wurzelgesetz der inneren Reibung starker Elektrolyte. *Z. Phys. Chem.* **6B**, 159–162 (1929). <https://doi.org/10.1515/zpch-1929-0618>
6. G. Jones, M. Dole, The viscosity of aqueous solutions of strong electrolytes with special reference to barium chloride. *J. Am. Chem. Soc.* **51**, 2950–2964 (1929). <https://doi.org/10.1021/ja01385a012>
7. M. Kaminsky, Experimentelle Untersuchungen über die Konzentrations- und Temperaturabhängigkeit der Zähigkeit wässriger Lösungen starker Elektrolyte. *Z. Phys. Chem.* **12**, 206–231 (1957). https://doi.org/10.1524/zpch.1957.12.3_4.206
8. J. Jiang, S.I. Sandler, A new model for the viscosity of electrolyte solutions. *Ind. Eng. Chem. Res.* **42**, 6267–6272 (2003). <https://doi.org/10.1021/ie0210659>
9. R.J. Lee, R.M. DiGiulio, S.M. Jeter, A.S. Teja, Properties of lithium bromide-water solutions at high temperatures and concentrations—II: density and viscosity. *ASHRAE Trans.* **96**, 3381 (1990)
10. K.E. Herold, R. Radermacher, S.A. Klein, *Absorption Chillers and Heat Pumps*, 1st edn. (CRC Press, Boca Raton, FL, 1995)

11. K.E. Herold, R. Radermacher, S.A. Klein, *Absorption Chillers and Heat Pumps*, 2nd edn. (CRC Press, Boca Raton, FL, 2016). <https://doi.org/10.1201/b19625>
12. F-Chart, LiBrSSC (aqueous lithium bromide) property routines (2021), http://fchart.com/ees/libr_help/ssclibr.pdf
13. D.S. Kim, C. Infante Ferreira, Air-cooled solar absorption air conditioning. Technical report BSE-NEO 0268.02.03.04.0008 (Delft University of Technology, 2005)
14. KCE ThermoFluidProperties. LibWaLi. <https://thermofluidprop.com/en/property-libraries/refrigerants-refrigerant-mixtures-and-coolants#c367>. Accessed 27 Sept 2022
15. Y. Cao, Y. Ding, Y. Guo, C. Wang, Y. Liu, L. Tao, J. Li, Measurement and calculations of density, viscosity and surface tension for lithium bromide and ionic liquid aqueous solutions. *CIESC J.* **72**, 1874–1884 (2021). <https://doi.org/10.11949/0438-1157.20201138>
16. S. Hasaba, T. Uemura, H. Narita, On the thermodynamic properties of aqueous lithium bromide solutions -2-. *Refrigeration* **36**, 4–11 (1961)
17. H. Löwer, Thermodynamische und physikalische Eigenschaften der wässrigen Lithiumbromidlösung. PhD Thesis, Technische Hochschule Karlsruhe, 1960
18. A. Lo Surdo, H. E. Wirth, Transport properties of aqueous electrolyte solutions. Temperature and concentration dependence of the conductance and viscosity of concentrated solutions of tetraalkylammonium bromides, ammonium bromide, and lithium bromide. *J. Phys. Chem.* **83**, 879–888 (1979). <https://doi.org/10.1021/j100470a024>
19. V.P. Mashovets, N.M. Baron, M.U. Scherba, Viscosity and density of aqueous LiCl, LiBr and LiI solutions at moderate and low temperatures. *J. Appl. Chem.* **44**, 1981–1986 (1971). [USSR: Transl. from Russian]
20. W. Raatschen, Thermophysikalische Eigenschaften von Methanol/Wasser - Lithiumbromid Lösungen. PhD Thesis (RWTH Aachen, 1985)
21. N. Rohman, N.N. Dass, S. Mahiuddin, Isentropic compressibility, effective pressure, classical sound absorption and shear relaxation time of aqueous lithium bromide, sodium bromide and potassium bromide solutions. *J. Mol. Liq.* **100**, 265–290 (2002). [https://doi.org/10.1016/S0167-7322\(02\)00047-8](https://doi.org/10.1016/S0167-7322(02)00047-8)
22. T. Satoh, K. Hayashi, The viscosity of concentrated aqueous solutions of strong electrolytes. *Bull. Chem. Soc. Jpn.* **34**, 1260–1264 (1961). <https://doi.org/10.1246/bcsj.34.1260>
23. J. M. Wimby, T. S. Berntsson, Viscosity and density of aqueous solutions of lithium bromide, lithium chloride, zinc bromide, calcium chloride and lithium nitrate. 1. Single salt solutions. *J. Chem. Eng. Data* **39**, 68–72 (1994). <https://doi.org/10.1021/jc00013a019>
24. T. Uemura, Physical properties of refrigerant-absorbent system for absorption refrigeration system. *Refrigeration* **52**, 65–76 (1977). <https://doi.org/10.11501/3291511>
25. I.D. Zaytsev, G.G. Aseyev (eds.), *Properties of Aqueous Solutions of Electrolytes* (CRC Press, Boca Raton, FL, 1992)
26. V.M. Valyashko (ed.), *Hydrothermal Properties of Materials* (Wiley, Chichester, 2008). <https://doi.org/10.1002/9780470094679>
27. A. Rohatgi, WebPlotDigitizer: version 4.3 (2020), <https://automeris.io/WebPlotDigitizer>
28. J. Pátek, J. Klomfar, Solid–liquid phase equilibrium in the systems of LiBr–H₂O and LiCl–H₂O. *Fluid Phase Equilib.* **250**, 138–149 (2006). <https://doi.org/10.1016/j.fluid.2006.09.005>
29. W. Wagner, A. Pruss, International equations for the saturation properties of ordinary water substance. Revised according to the international temperature scale of 1990. Addendum to *J. Phys. Chem. Ref. Data* **16**, 893 (1987). *J. Phys. Chem. Ref. Data* **22**, 783–787 (1993). <https://doi.org/10.1063/1.555926>
30. The MathWorks Inc., *MATLAB R2022b Curve Fitting Toolbox* (The MathWorks Inc., Natick, MA, 2022), <https://www.mathworks.com/help/curvefit/>
31. Y. Dodge, *The Concise Encyclopedia of Statistics* (Springer, New York, NY, 2008), pp.299–302. https://doi.org/10.1007/978-0-387-32833-1_225
32. A. Field, *Discovering Statistics Using IBM SPSS Statistics* (Sage Publications Ltd, London, 2018)
33. IAPWS, Release on the IAPWS Formulation 2008 for the viscosity of ordinary water substance. Technical report IAPWS R12-08 (The International Association for the Properties of Water and Steam, 2008), <http://www.iapws.org/relguide/viscosity.html>
34. M.L. Huber, R.A. Perkins, A. Laesecke, D.G. Friend, J.V. Sengers, M.J. Assael, I.N. Metaxa, E. Vogel, R. Mareš, K. Miyagawa, New international formulation for the viscosity of H₂O. *J. Phys. Chem. Ref. Data* **38**, 101–125 (2009). <https://doi.org/10.1063/1.3088050>
35. IAPWS, Revised release on the IAPWS formulation 1995 for the thermodynamic properties of ordinary water substance for general and scientific use. Technical report IAPWS R6-95(2018) (The International

- Association for the Properties of Water and Steam, 2018), <http://www.iapws.org/relguide/IAPWS-95.html>
36. W. Wagner, A. Pruß, The IAPWS formulation 1995 for the thermodynamic properties of ordinary water substance for general and scientific use. *J. Phys. Chem. Ref. Data* **31**, 387–535 (2002). <https://doi.org/10.1063/1.1461829>
 37. P. Junglas, WATER95—a MATLAB® implementation of the IAPWS-95 standard for use in thermodynamics lectures. *Int. J. Eng. Educ.* **25**, 3–10 (2009)
 38. D. Kim, C. Infante Ferreira, A Gibbs energy equation for LiBr aqueous solutions. *Int. J. Refrig.* **29**, 36–46 (2006). <https://doi.org/10.1016/j.ijrefrig.2005.05.006>

Publisher's Note Springer Nature remains neutral with regard to jurisdictional claims in published maps and institutional affiliations.